

**IMPROVED EVENT LOCATION UNCERTAINTY ESTIMATES**

István Bondár, Keith McLaughlin, and Hans Israelsson

Science Applications International Corporation

Sponsored by Air Force Research Laboratory

Contract No. FA8718-05-C-0018

**ABSTRACT**

The objectives of this project are to develop, test, and validate methodologies that improve location uncertainties in the presence of correlated, systematic model errors and non-Gaussian measurement errors. Un-modeled lateral heterogeneity in the Earth introduces systematic correlated travel-time errors that bias locations derived from unbalanced networks. Furthermore, emergent arrivals, noise bursts, and other blunders introduce non-Gaussian errors not properly modeled by standard least-squares location procedures.

In the previous year we presented a method based on copula theory to estimate the spatial correlation structure in arrival-time data. Based on these models, we have incorporated the full covariance matrix weighting into a standard linearized least-squares location algorithm. We have developed and validated generic variogram models (regional and teleseismic) using globally distributed clusters of GT5 events identified by the Global Ground Truth project (FA8718-4-C-0020). These models may be used as conservative correlation estimators to generate the full data covariance matrix for regions where there are insufficient data to estimate a variogram. We have demonstrated improvements in both locations and uncertainty estimates by accounting for correlated, Gaussian errors. While un-modeled location biases remain, location estimates are less sensitive to unbalanced network configurations. Coverage statistics are significantly improved for a wide range of number of defining phases with the improved error ellipses.

We have refined and tested our signal-to-noise ratio (SNR)-based measurement error model and developed a measurement error model using body wave magnitude (mb) as a substitute for SNR. We have incorporated both measurement error models into our standard linearized iterative least-squares algorithm. The increased variance and bias (late pick) for small events is quantified as a family of distributions dependent upon observed or expected SNR. Since the measurement errors now describe a non-Gaussian model, the standard least-squares location algorithm may no longer be optimal.

Our research now focuses on exploring alternative objective functions ( $l_p$ -norms) and regression algorithms that exploit both the spatial correlation models and the new non-Gaussian error models for improved location uncertainties. We show Monte Carlo comparisons contrasting Gaussian and non-Gaussian skewed distributions. A preliminary network geometry stability or quality criteria is proposed that predicts the sensitivity to non-Gaussian errors.

**OBJECTIVES**

The objectives of this project are to develop methodologies to estimate location uncertainties in the presence of correlated, systematic model errors and to characterize non-Gaussian measurement errors as a function of signal parameters such as SNR or network magnitude, a surrogate for SNR. The improved understanding of a correlated Gaussian error budget described by a full covariance matrix is now incorporated into a linearized location algorithm leading to more robust estimates of location uncertainty. The ultimate goal of this project is to develop transportable Gaussian and non-Gaussian error models that will provide reliable location uncertainty estimates for small events recorded by sparse or dense, balanced or imbalanced networks.

**RESEARCH ACCOMPLISHED**

The motivation for this project is the observation that location uncertainty estimates are often underestimated; error ellipses scaled to the 90% confidence level do not contain 90% of the true locations. This is due to violation of the assumptions of normally distributed independent observations commonly made by standard linearized location algorithms. Due to unaccounted velocity heterogeneities, similar ray paths produce systematic travel-time prediction errors and lead to correlated error structures. Furthermore, picking residuals are non-Gaussian and better described by skewed, heavy-tailed distributions. Phase picks suffer from systematic errors as onset times along the same ray paths are systematically picked late with decreasing event size, or more precisely, with decreasing SNR (e.g., Douglas et al., 1997, 2005a, 2005b). Douglas et al. (2005a) point out that automatic detections are more likely affected by the systematic errors than are manual picks made by experienced analysts. These systematic reading errors introduce location biases for smaller events.

In this project we focus on the treatment of correlated errors combined with non-Gaussian, non-zero-mean, heavy-tailed, skewed distributions of reading errors. Figure 1 illustrates our research strategy. During the first year of the project (Bondár et al., 2006a), we developed a new, copula-based methodology to estimate variograms. The variogram models were used to construct the network covariance matrix, which describes the correlated travel-time structure due to un-modeled path effects along similar ray paths. We incorporated the full data covariance matrix into an existing linearized iterative least-squares (ILS) algorithm and demonstrated improvements both in location and coverage with increasing numbers of defining phases or imbalanced networks. This year we concentrated our efforts on developing improved models of picking error bias and variance as a function of SNR and network magnitude. By exploiting new ground truth events produced by our related GT project (Bondár et al., 2007), we have developed generic, transportable variogram models for regional Pn and teleseismic P phases that can be used to construct network covariance matrices anywhere on the globe.

<i>Baseline</i>		<i>Year 1</i>		<i>Year 2</i>		<i>Year 3</i>	
<i>Pick Error</i>	<i>Model Error</i>	<i>Pick Error</i>	<i>Model Error</i>	<i>Pick Error</i>	<i>Model Error</i>	<i>Pick Error</i>	<i>Model Error</i>
Normal IID	Normal IID	Normal IID	Correlated Normal  Specific variogram models	Non-Normal  SNR/mb dependent bias and variance	Correlated Normal  Generic variogram models	Non-Normal  SNR/mb dependent bias and variance	Correlated Normal  Generic variogram models
<b>Linearized ILS inversion (diagonal covariance matrix)</b>		<b>Linearized ILS inversion with full covariance matrix</b>		<b>Linearized ILS inversion with correlated errors with full covariance matrix and pick bias as travel-time correction</b>		<b>Monte Carlo-based hypothesis tests with correlated errors—validity of coverage ellipse given linearized approach—alternative Lp norms</b>	

**Figure 1. Progress and strategy of research. Gray indicates existing state of the art, Green completed work, and Yellow future work. Year 1 culminated in an ILS algorithm that utilized a full covariance matrix based on new variogram models for improved location uncertainty. Year 2 completed validation tests for implementation of new picking error models and new generic variogram models.**

**Measurement Error Models**

It has long been noted that arrival time errors depend on SNR (Freedman, 1966; Lomnitz, 1995). Low SNR arrival times tend to be read late and have increasing variance (Douglas et al., 2005b). Lateness in low SNR readings is not accounted for in standard locations of seismic events. However, arrival times for a given event read at stations with varying SNRs may, as Douglas et al. (2005b) point out, contribute to bias in the epicenter estimate. Delays in arrival readings have not been accounted for simply due to lack of reported SNR. Indeed, as Douglas et al. (2005b) observe, few actual estimates of reading error characteristics—delay, variance, distributions - have been published. Digital recording with associated automatic processing affords opportunities to characterize reading errors as a function of SNR as well as other signal attributes. For example, the International Data Centre (IDC) employs *a priori* variances for arrival time variance as a function of SNR—for both automatic and analyst picks; the SNR is defined as the ratio of the short-term average/long-term average of the detecting beam. The IDC makes, however, no assumption about lateness or bias in arrival times. Figure 2 illustrates that once path effects are removed, a trend of increasingly late picks with decreasing event size emerges.

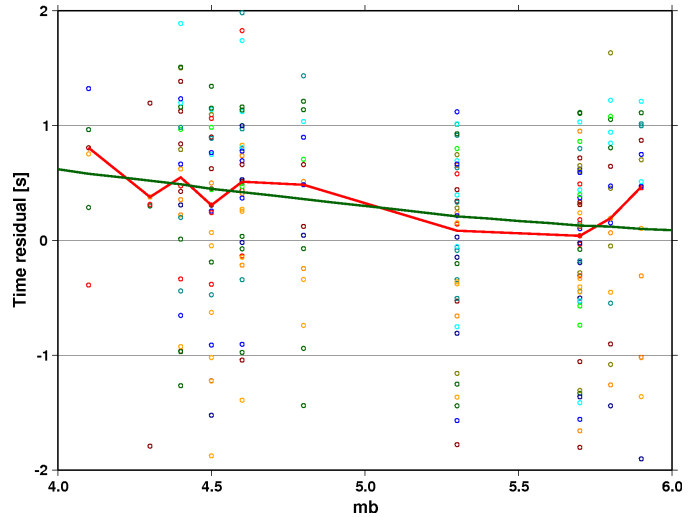


**Figure 2. Median Pn station residuals with regard to GT0 locations of Yucca Flat explosions from CUB2 model predictions. Picks are systematically late with decreasing event size.**

*SNR-based picking error model*

Our goal is to develop improved models of both bias and variance in reading errors as a function of SNR. To accomplish this goal, we follow a double-difference approach. We assume that arrival times with corresponding SNR estimates from a network of stations are available from an event cluster of GT events. We write the arrival time at station *i* from event *x* as  $t_{ix} = OT_x + t_{ix}^{pred} + t_i^{path} + t_{ix}^{delay} + \epsilon_{ix}$ , where  $OT_x$  is the origin time of event *x*,  $t_{ix}^{pred}$  is the predicted (IASPEI91) travel time,  $t_i^{path}$  is the path effect (station term),  $t_{ix}^{delay}$  is the pick delay and  $\epsilon_{ix}$  is a random picking error. We assume only  $t_{ix}^{delay}$  and  $\epsilon_{ix}$  are functions of  $SNR_{ix}$ . By forming selected double differences, the origin times and systematic station terms may be canceled:

$$(t_{ix} - t_{iy}) - (t_{jx} - t_{jy}) - (t_{ix}^{pred} - t_{iy}^{pred}) + (t_{jx}^{pred} - t_{jy}^{pred}) = (t_{ix}^{delay} - t_{iy}^{delay}) - (t_{jx}^{delay} - t_{jy}^{delay}) + (\epsilon_{ix} - \epsilon_{iy}) - (\epsilon_{jx} - \epsilon_{jy})$$

The right hand side of the equation can be calculated from the observed arrival times and the predicted travel times. The mean delay and the total variance (assuming that the travel-time prediction errors are more or less the same) are written as  $\mu^{delay}(SNR) = (t_{ix}^{delay} - t_{iy}^{delay}) - (t_{jx}^{delay} - t_{jy}^{delay})$ , and

$$Var^{total} = 4Var_{hypo} + Var(SNR_{ix}) + Var(SNR_{iy}) + Var(SNR_{jx}) + Var(SNR_{jy}).$$

For sufficiently large SNR values we assume the pick delay and its variance approach zero. Thus, if all four readings have large SNR, the total variance gives us an estimate of the model error variance. This allows us to get an estimate of the variance of reading errors when all four readings have small SNR:

$Var(SNR) \rightarrow (Var^{total} - 4Var_{hypo}^{largeSNR}) / 4$ . Now let us presume that three of the readings have large SNR, and one has a small SNR. Then the mean delay simply becomes  $\mu^{delay}(SNR) \rightarrow t^{delay(SNR_{small})}$ . Hence, the double-difference (DD) approach, with proper data selection, provides a methodology to derive models of bias and variance in picking errors.

To establish SNR-dependent models of delay and variance, we used first-arriving P from 12 HDC-RCA clusters (see Bondár et al., 2006b, 2007) with  $SNR \geq 3$  reported in the PIDC/IDC REB. We calculated all possible DDs in

each cluster and selected two subsets for each cluster. One subset consisted of the DD residuals for which the SNRs of all four arrivals were within a factor of 2. Figure 3a shows the DD residuals for this subset as a function of median SNR, as well as the scaled median absolute deviation (SMAD) of residuals along moving SNR windows. The other subset included DD residuals with the three largest SNR  $\geq 40$ . The DD residuals are plotted as a function of minimum SNR in Figure 3b. The running median (dashed curve) is the estimate of reading error bias as a function of SNR.

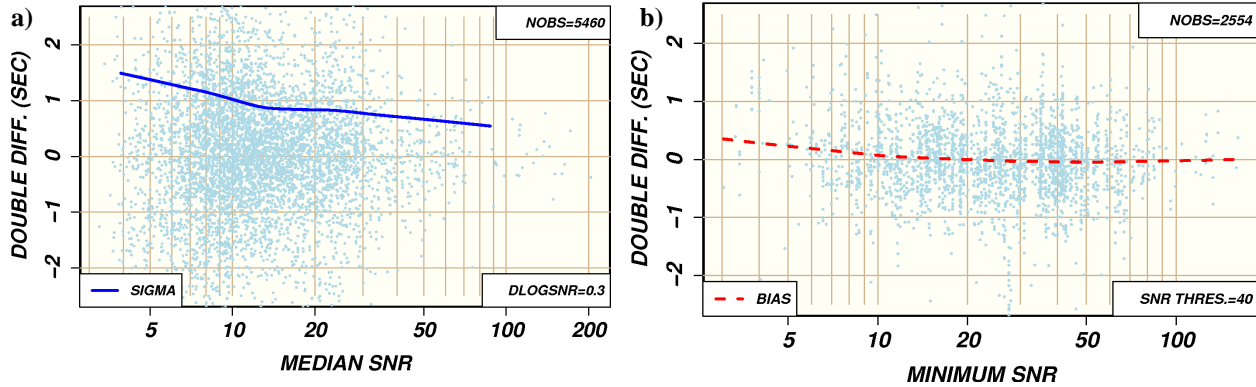


Figure 3. a) DD residuals where all four SNR are similar. The running SMAD (blue curve) represents the estimate of total variance. b) DD residuals where the SNR of three arrivals is large and the SNR of one arrival is small. The running median (red) provides an estimate of the reading error bias.

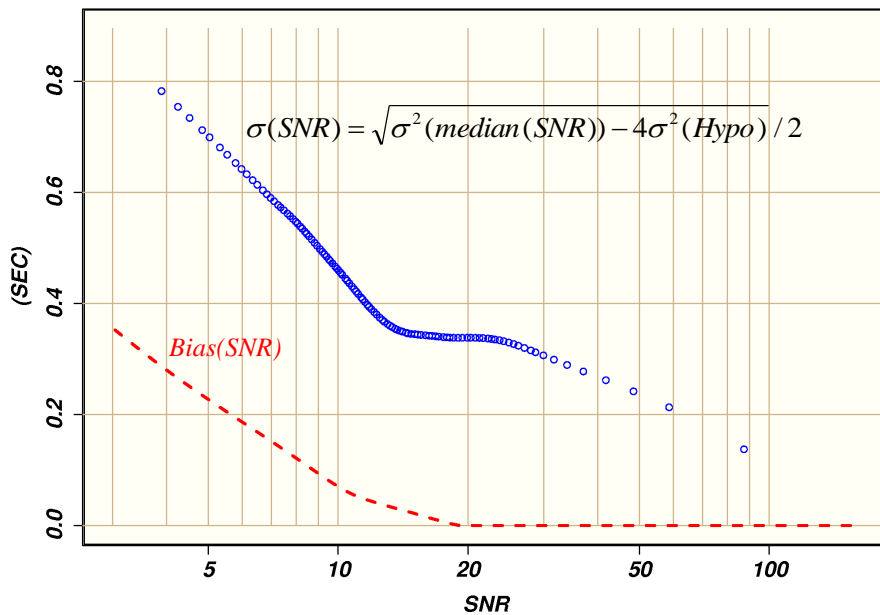


Figure 4. SNR-dependent model for pick delay and standard deviation.

Recall that the running SMAD in Figure 3a is an estimate of the total variance in the DD residuals which includes the background variance of travel-time prediction errors. We estimate  $Var_{hypo}$  from the second subset as the variance of DD residuals where the minimum SNR is larger than 40. This gives us an estimate  $\sigma_{Hypo} = 0.24s$  which has to be removed from the total variance estimates in order to get an estimate of the reading error variance. Our resulting model for reading error bias and variance is shown in Figure 4.

In the linearized ILS location algorithm the bias is implemented as a travel-time correction, while the variance is added to the main diagonal of the network covariance matrix.

Note that the International Monitoring Station (IMS) being a sparse, teleseismic network, the SNR-based measurement error model is dominated by teleseismic P phases, which explains the relatively small delays even at very low SNR values. As Figure 2 suggests, delays are expected to be much larger for regional phases.

*The mb-based picking error model*

Currently only the IDC Reviewed Event Bulletin reports SNR estimates for arrival picks, and as we indicated above, there is insufficient data to derive SNR-based error models for phases other than teleseismic P. Thus, the SNR-based error model has a very limited scope for practical application. To develop a measurement error model that can be

used for the vast majority of events with no reported SNR estimates of phase arrivals, we decided to use network magnitude as a surrogate for SNR. Network magnitude is admittedly a crude surrogate for mb, but at least it is reported for most events.

We used events from Yucca Flat and Pahute Mesa with network magnitudes ( $4 < mb < 6$ ) reported in the International Seismological Centre (ISC) bulletin to derive mb-based models of reading error bias and variance. We fit the measurement error model for first-arriving P phases as a smooth function of epicentral distance and mb. Figure 5 shows our mb distance based model. Not surprisingly, the picking delay is largest at far regional distances. For teleseismic distances, the bias estimates are smaller and show good agreement with those predicted by the SNR-based model.

Figure 5 suggests that the effect of phase pick delays on event locations with decreasing magnitude may be negligible for teleseismic networks, but cannot be ignored for local and regional stations. Note that the mb-based measurement error model assumes that path effects are largely accounted for; therefore they should properly be used in conjunction with source-specific station corrections (SSSCs) or other path corrections.

Figure 6 shows relocations of GT0-2 explosions from various event clusters with and without SSSCs and mb-delay corrections using regional Pn only. The SSSCs were calculated from CUB2 (Shapiro and Ritzwoller, 2004) travel-time predictions relative to IASPEI91 (Kennett and Engdahl, 1991) predictions. The calibrated travel times are primarily responsible for location improvements, although they suffer from some remaining regional biases. The effect of mb-delay corrections is less obvious, but nonetheless significant. The amplitude of the mb-delay corrections is much smaller than those from the SSSCs; therefore, they only move events by 1 or 2 kilometers maximum which is typically less than the accuracy of the GT0-2 event locations. However, they do tend to tighten event clusters, by moving smaller events closer to larger ones.

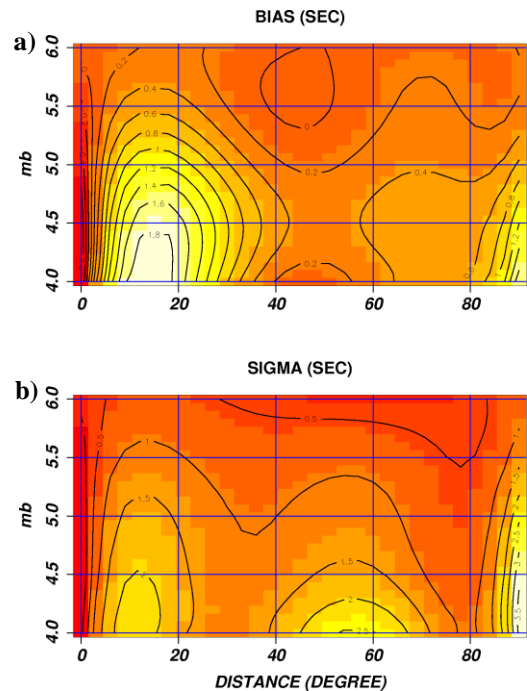


Figure 5. An mb-based model of bias (a) and variance (b) for reading errors.

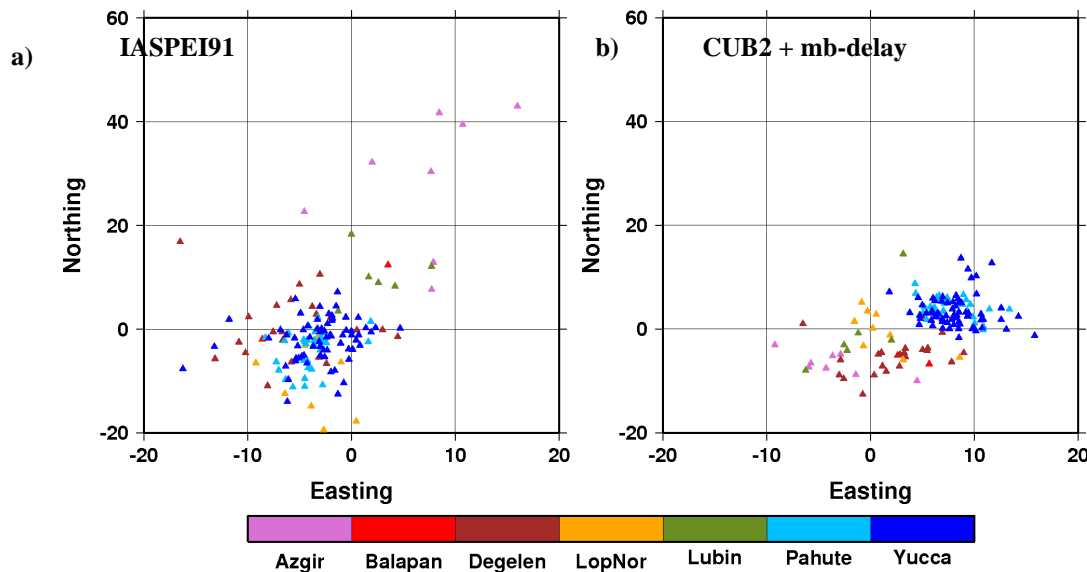
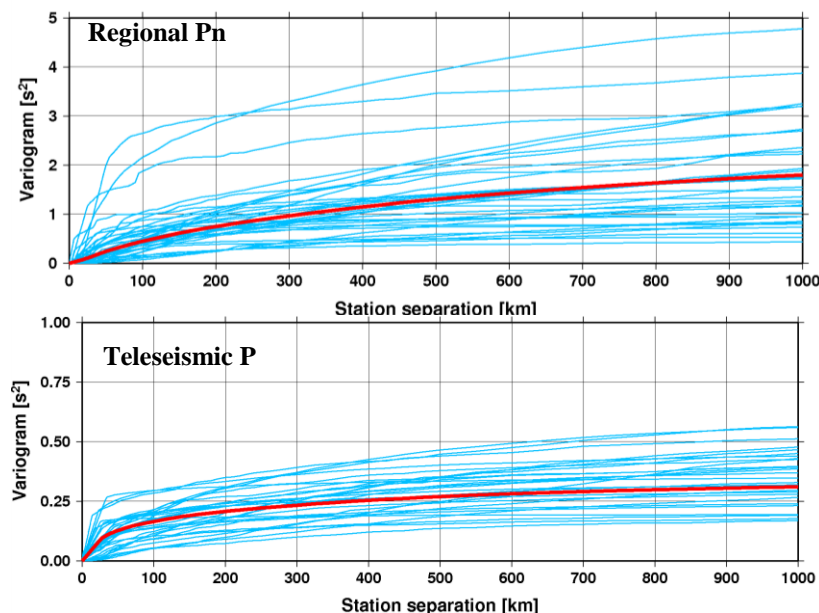


Figure 6. Relocation of GT0-2 event clusters using a) IASPEI91 baseline travel times and b) CUB2 travel-time predictions with mb-based delay and variance model. Events are colored according to

their cluster. Individual clusters tend to individually coalesce with application of the CUB2 and mb-delay corrections.

### Generic Variogram Models

Last year we demonstrated utility of source region specific teleseismic P and Pn correlation structures. Nearly all source region specific teleseismic P variograms were similar and could generally be interchanged. Pn variograms



**Figure 7. Variogram models for all GT clusters from the Global GT project (Bondár et al., 2007). The generic variogram model derived from all data is shown in red.**

models indeed account for major 3D heterogeneities. Consistent with previous results the calibrations reduced the overall variance (the sill) by just under 50%. Nevertheless, un-modeled velocity structures remain that generate correlated travel-time residuals. Because the calibrated travel times now account for the bulk of 3D Earth structure, it allows us to derive an isotropic variogram model not just from the individual clusters, but from the entire data set of globally distributed GT5 or better events. These models, shown as red lines on Figure 7, define generic Pn and P variograms that can be used to construct network covariance matrices for calibrated regions.

### Validation Tests

To validate the generic calibrated error models (described by the network covariance matrix we generate from the transportable variogram models) as well as the mb/SNR-dependent delay correction and measurement error models we used over 2,000 globally distributed GT5 or better events produced under the Global GT project (Bondár et al., 2007). The regional and teleseismic ISC station coverage varies from sparse to dense networks for these clusters. To locate events we used our ILS location algorithm (Bondár et al., 2006a) developed in Year 1 that uses the full data covariance matrix to take into account the correlated structure in the travel times. Calibrated travel-time corrections, i.e., SSSCs, were generated from the CUB2 (Shapiro and Ritzwoller, 2004) and Harvard (Antolik et al., 2003) global 3D models for Pn and P, respectively. Figure 8 shows the mislocations relative to the GT5 locations for four test cases. Figure 9 shows cumulatives of mislocation, 90% error ellipse area, and coverage for three test cases. And, Figure 10 compares results at two clusters for two test cases. Calibrated travel-times, i.e., SSSCs, provide the first-order effect in location improvements for events mislocated significantly more than their GT level (visually in Figure 8 and bottom panel Figure 9). Taking into account the residual correlated data structure improves coverage (top panel Figure 9) with incremental improvements in locations. The mb-based picking error model tightens some of the clusters with a large range of magnitudes (Figure 10).

demonstrated more diversity with source region and could not be interchanged. We additionally showed that once the bulk of the path effects are removed by calibration, it is possible to develop generic, transportable variogram models for both teleseismic P and Pn that may work well anywhere on the globe. We calculated Pn and P variogram models using our copula methodology (Bondár et al., 2006a) for all GT5 clusters from the global GT project (Bondár et al., 2007). For Pn and P calibration we used CUB2 (Shapiro and Ritzwoller, 2004) and Harvard (Antolik et al., 2003) SSSCs, respectively. Figure 7 shows the Pn and P variogram models obtained from GT residuals after calibration. The fact that the variograms look quite similar indicates that the CUB2 and Harvard global 3D

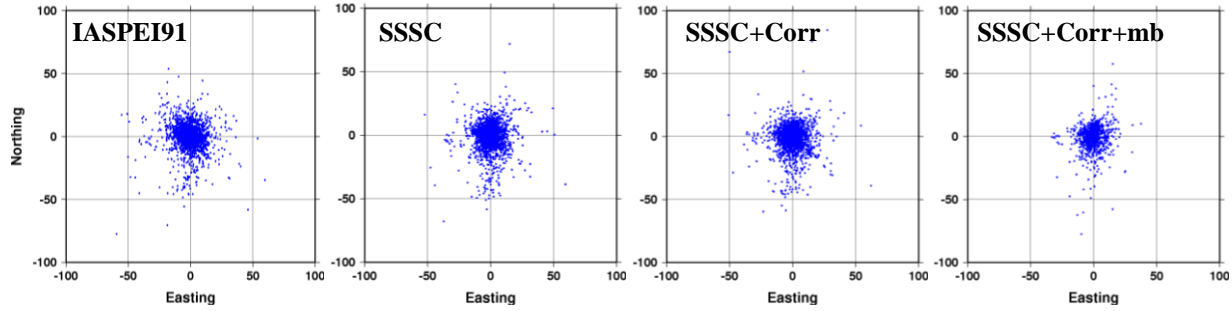


Figure 8. Relocations of over 2,000 globally distributed GT5 or better events with a) IASPEI91, b) SSSCs, c) SSSCs and full data covariance matrix, and d) SSSCs and full data covariance matrix and mb-based delay corrections and variances (a subset of events from a, b and c with  $4 \leq mb \leq 6$ ).

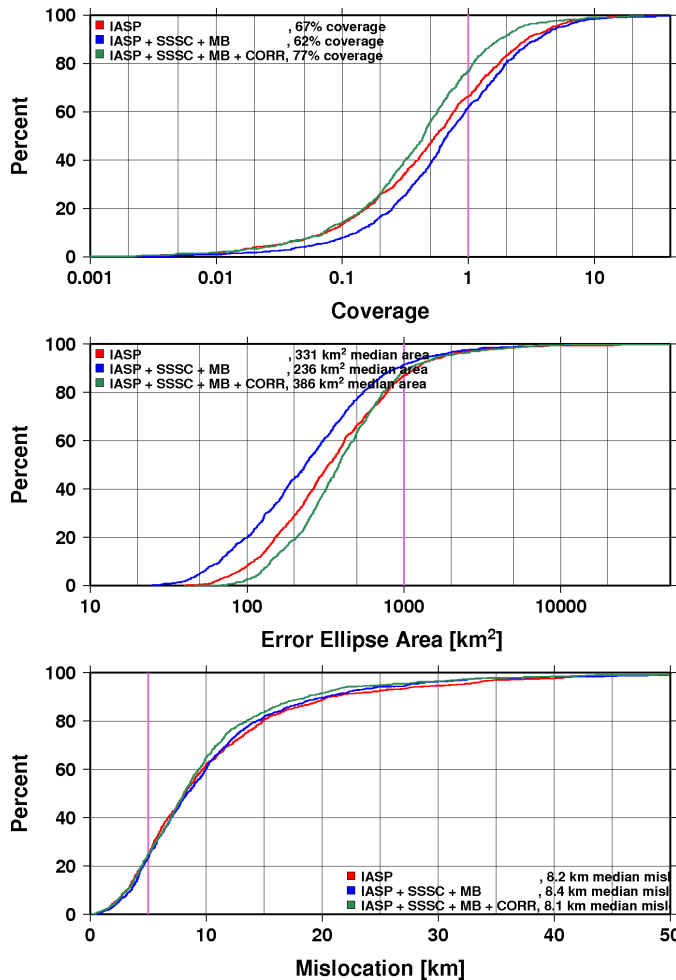
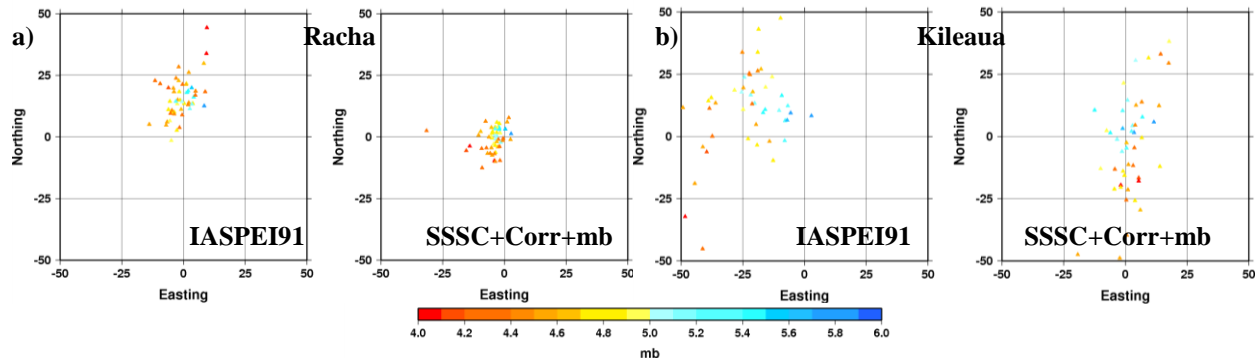


Figure 9. Cumulative distributions of mislocation (bottom panel), error ellipse area (middle panel) and coverage (top panel) for events with  $4 \leq mb \leq 6$  with IASPEI91 (red), SSSCs and mb-based delay corrections and variances (blue) and with correlated error structure (green).

Figure 9 shows cumulative distributions for mislocation, error ellipse area and coverage for 945 events with  $4 \leq mb \leq 6$  (the magnitude range where the mb-delay corrections and mb-variances are currently defined). Recall that the mb-based error models (blue) of bias and variance were derived from an explosion data set. These mb-dependent measurement error estimates may be too optimistic for earthquakes, which may explain why the area of the error ellipses is underestimated and insufficient coverage. While the median mislocations remain more or less the same, the generic correlated error model (shown in green) provides systematic location improvements above the 60th percentile (or mislocations exceeding 10 km). More important, taking into account the correlated structure, using the transportable Pn and P correlated error models increases the coverage from about 60% to 80% without significant inflation of the error ellipses. A small increase in the variogram sill would assure 90% coverage.

Figure 10 shows relocations for the Racha, Caucas and the Kileaua, Hawaii GT5 clusters. Events are colored by their network magnitude and show internal clustering of large and small events. The new models appear to tighten the clusters by reducing the systematic location discrepancy between the small and large events. The net centroid bias is also reduced for both these clusters.



**Figure 10. Location errors (eastings and northings in km) relative to GT5 locations without (IASPEI91) and with calibrated travel-times, mb-delay corrections and correlated errors for a) Racha, Caucasus cluster and b) Kileaua, Hawaii cluster. Events are colored according to their mb ( $4 < mb < 6$ ). Disparities between large (redish) and small (blueish) events are reduced.**

To test the SNR-based measurement error model, we used only those arrivals with reported SNR estimates. This basically restricted our globally distributed GT5 events to those that appear in the prototype IDC/IDC REB. As we mentioned earlier, the SNR-based delay and variance estimates are largely limited to teleseismic P, for which the delay correction is quite modest. There are indications that the SNR-based delay corrections make the clusters slightly tighter but the relocation tests are largely inconclusive and do not demonstrate significant improvements (or degradation). The transportable generic variogram models achieve the same coverage level (about 80%) for the sparse IMS network, indicating the same small sill adjustment to the variogram model is in order.

## **CONCLUSIONS AND RECOMMENDATIONS**

We have developed generic transportable variogram models for Pn and P phases. By relocating a data set of globally distributed GT5 or better events, we demonstrated that the transportable variogram models used to construct network covariance matrices account for correlated structure in travel-time predictions and achieve 80% coverage for both sparse and dense networks. While we are still a bit shy of the nominal 90% coverage expected from the error ellipses scaled to the 90% confidence level, the models require only minor fine tuning to achieve actual 90% coverage.

We have developed a DD-based methodology to derive SNR-dependent models of bias and variance for reading errors. Since SNR estimates are rarely reported, we prototyped measurement error models of phase pick delay and variance using network magnitude. Admittedly, mb is a rudimentary surrogate for SNR but it is reported for most events. While the phenomenon that arrivals picked increasingly late with decreasing event size is well established (especially for automatic picks), so far little effort has been made to account for the systematic lateness of picks in a standard location algorithm. We implemented the SNR/mb-dependent bias estimates as travel-time corrections in our location algorithm. Application of the delay correction assumes that calibrated travel times are used. The SNR/mb-dependent phase pick variances are added to the diagonals of the network covariance matrix. The validation tests have shown that the effect of phase pick delay corrections is second order relative to calibrated travel-times. The phase pick delay corrections typically move locations less than the accuracy of our GT test events. Nevertheless, the error model improves some event patterns by reducing the systematic location discrepancy between small and large events, thus making the event clusters tighter.

As indicated in Table 1, our research now focuses on exploring alternative objective functions ( $l_p$ -norms), regression algorithms, and hypothesis tests to account for input travel-time errors with un-modeled spatial correlation and non-Gaussian picking errors. For example, the results of a simple Monte Carlo experiment are shown in Figure 11. Random local networks (10 stations with epicentral distances  $< 150$  km) were chosen and assigned random errors drawn from Gaussian, Weibull, and Gumbel distributions (all with zero mean and standard deviation 1 s). The resulting distribution of mislocations from the input non-Gaussian errors are well described by the Normal model below the 80th percentile. However at the higher percentiles, the Gumbel and Weibull input skewed tails are poorly modeled by the Gaussian distribution. We found that deviations from a Normal model could be predicted by a simple Location Quality metric defined as  $QL = (1 - azgap/360)(1 - sazgap/360)$  where azgap and sazgap are the primary and secondary azimuthal gaps of the network. Figure 12 shows median and 95th percentiles location errors as a function of QL and it is clear that when QL exceeds 1/2 the network deviates from Normal. Simulations such as

these suggest the utility of stability tests based on network geometry for judging the validity of the Normal model for location uncertainty estimation.

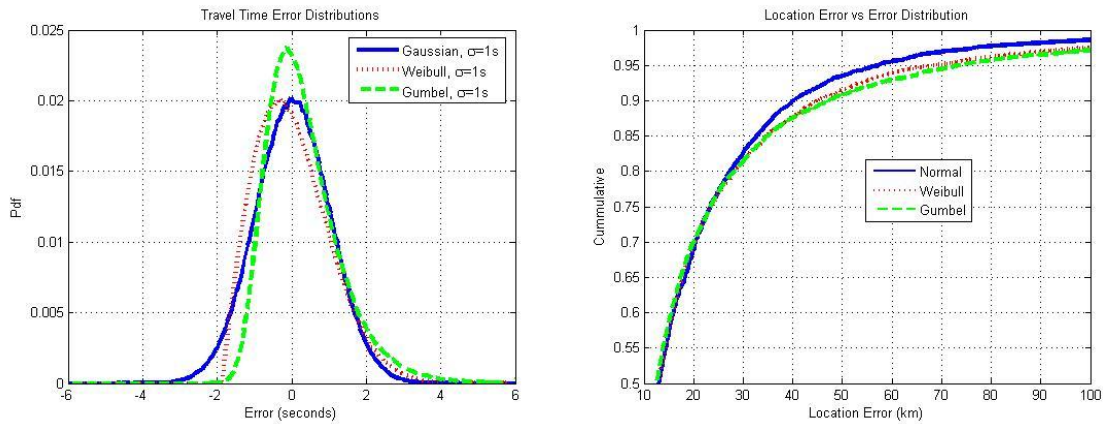


Figure 11. Gaussian, Weibull, and Gumbel input error distributions (each zero mean and 1 s standard deviation) were used in a Monte Carlo location experiment. Mislocations resulting from non-Gaussian input errors are under predicted by the Normal model above the 80th percentile.

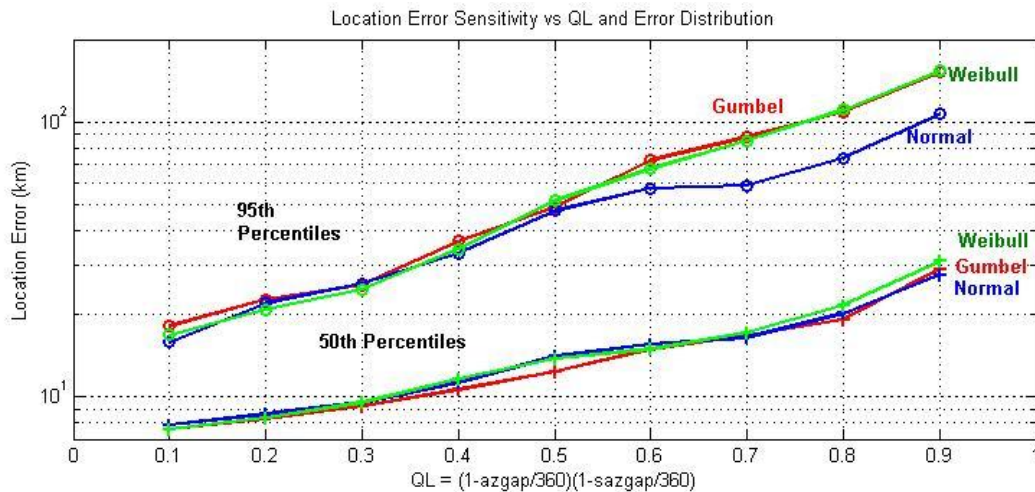


Figure 12. Deviations from the Normal model are greatest for poor network configurations described by QL. Small QL is good, while networks with large QL are potentially unstable.

**REFERENCES**

Antolik, M., Y.J. Gu, G. Ekström, and A. Dziewonski (2003). J362D28: A new joint model of compressional and shear velocities in the earth's mantle, *Geophys. J. Int.* 153: 443–466.

Bondár, I., K. McLaughlin, and H. Israelsson (2006a). Improved event location uncertainty estimates, in *Proceedings of the 28th Seismic Research Review: Ground-Based Nuclear Explosion Monitoring Technologies*, LA-UR-06-5471, Vol. 1, pp. 368–376.

Bondár, I., B. Kohl, E. Bergman, K. McLaughlin, H. Israelsson, Y-L. Kung, J. Given and E.R. Engdahl (2006b). Global ground truth data set with waveform and improved arrival data, in *Proceedings of the 28th Seismic Research Review: Ground-Based Nuclear Explosion Monitoring Technologies*, LA-UR-06-5471, Vol. 1, pp. 359–367.

## 29th Monitoring Research Review: Ground-Based Nuclear Explosion Monitoring Technologies

- Bondár, I., B. Kohl, E. Bergman, K. McLaughlin, Y-L. Kung, and E. R. Engdahl (2007). Global ground truth data set with waveform and improved arrival data, in current Proceedings.
- Douglas, A., D. Bowers and J. B. Young (1997). On the onset of P seismograms, *Geophys. J. Int.* 129: 681–690.
- Douglas, A., J.B. Young, D. Bowers and M. Lewis (2005a). Variation in reading error in P times for explosions with body-wave magnitude, *Phys. Earth Planet. Int.* 152: 1–6.
- Douglas, A., J. B. Young, D. Bowers and P. D. Marshall (2005b). An analysis of P travel times for Nevada Test Site explosions recorded at regional distances, *Bull. Seism. Soc. Am.* 95: 941–950.
- Freedman, H. W. (1966). A statistical discussion of Pn residuals from explosions, *Bull. Seism. Soc. Am.* 56: 677–695.
- Lomnitz, C. (1995). Comment on "Errors in hypocenter location: Picking, model, and magnitude dependence," by S. D. Billings, M. S. Sambridge, and B. L. N. Kennett, *Bull. Seism. Soc. Am.* 85: 1527–1528.
- Kennett, B. L. N. and E. R. Engdahl (1991). Travel times for global earthquake location and phase identification, *Geophys. J. Int.* 105: 429–465.
- Shapiro, N. M. and M. H. Ritzwoller (2004). Thermodynamic constraints on seismic inversions, *Geophys. J. Int.* 157: 1175–1188, doi:10.1111/j.1365-246X.2004.02254.x.